SciMedCentral

Journal of Dermatology and Clinical Research

Research Article

Comparison Between Hydrozincite and Zinc Oxide on The Healing of Deep Wounds Using a Rat Model

Osamu Yamamoto[1]* Yoshinori Nakayama[1], Miki Nagashima[1], Yoshimi Nakata[2], and Etsuro Udagawa[2]

[1]Graduate School of Science and Engineering, Yamagata University, Japan

[2]Research Laboratories, JFE Mineral & Alloy Co. Ltd, Japan

*Corresponding author

Osamu Yamamoto, Graduate School of Science and Engineering, Yamagata University, Japan, Tel: 81-238-26-3366

Submitted: 04 February 2023

Accepted: 13 February 2023

Published: 16 February 2023

ISSN: 2373-9371

Keywords

• Keywords: Ceramic; Powder; Wound healing; Regenerative skin

Abstract

According to the prescription of zinc oxide ointment for wound healing, the pharmacological actions of zinc oxide in the ointment are written to be wound astringent, anti-inflammatory, and antiseptic. There are various types of basic zinc compounds such as zinc oxide, and hydrozincite has been known as one of them. In this study, hydrozincite was proposed as a new wound-healing ceramic alternative to zinc oxide, and the effects of zinc oxide and hydrozincite on deep wound healing were compared using a rat model. The residual wound area of hydrozincite was significantly lower than that of zinc oxide and commercial wound dressing at 2 and 4 weeks of healing time. In histological evaluation, zinc oxide-applied wounds showed poor granulation and inflammatory cell infiltration for 1-2weeks, and zinc oxide powder remained in the poor granulation tissue. On the other hand, benign granulation tissue at which hydrozincite was applied to wounds was observed at 1 week with inflammatory cell infiltration. The inflammation ended after 2 weeks, and fibroblasts were observed in the regenerated skin tissue. From these results, hydrozincite was found to be a new candidate ceramic for wound healing alternative to zinc oxide.

INTRODUCTION

Zinc oxide ointments contain 20-50% ZnO powder and hydrophobic organic substances, which have been sold as Class 3 drugs for wounds in Japan for 60 years. To findings from the clinical practice of zinc oxide ointments, the pharmacological actions of ZnO based on prescription are wound astringent, anti-inflammatory, and antiseptic (antibacterial activity), etc., and it is believed that these actions are expressed by the binding of proteins at the wound site to ZnO [1,2]. According to the findings based on biology, activated mast cells release Zn^{2+} ions at the wound site, which acts on fibroblasts and then induces inflammatory cytokines such as interleukin-6 [3-6]. Inflammatory cytokines regulate the inflammatory phase of the wound healing process, and fibroblasts produce the protein collagen. Benign granulation is produced from angiogenesis and collagen. Finally, the wound is repaired via proliferative and remodeling phases. Regarding the above-mentioned, zinc oxide can be considered to have biological and pharmacological effects since zinc oxide dissolves slightly in water and releases Zn^{2+} ions. With respect to the action of metal ions on the wound healing of ceramics, wound-healing effects of Zn^{2+} and Si^{4+} ions have been also reported in Zn-smectite [7]. Contemplating the involvement of Zn^{2+} ions in wound healing mentioned above, it is not sure whether zinc oxide is optimal for these effects on wound healing or not. Several basic ceramics can be presumed to have similar effects to zinc oxide, one of which is hydrozincite.

Hydrozincite is an ion-bonding ceramic containing zinc ions, carbonate, and hydroxyl groups. Validation of the wound healing effect between zinc oxide and hydrozincite is important for the application of ceramics to medicine. The aim of the present work is to compare the wound healing effects between medicinal zinc oxide and hydrozincite using a rat model and to clarify the effectiveness of hydrozincite.

MATERIAL AND METHODS

Powder sample in this study

A commercially medicinal zinc oxide powder (hereafter ZnO: Nacalai Tesque, Kyoto, Japan) was used in this work. The powder samples were sterilized in an autoclave at 180°C for 20 min. The procedure for the synthesis of hydrozincite is as follows: The aqueous solution of zinc sulphate (Nacalai Tesque, Kyoto, Japan) was added dropwise into the aqueous solution of sodium bicarbonate (Nacalai Tesque, Kyoto, Japan). Sodium hydroxide aqueous solution with a concentration of 0.1 mol/L (Nacalai Tesque, Kyoto, Japan) was used in a timely manner to maintain the pH at 6.5. The precipitate obtained at pH 6.5 was washed with distilled water three times and then dried under a vacuum. The dried precipitate was sterilized by UV irradiation for 48 h, and a crystalline hydrozincite (hereafter $Zn_5(CO_3)_2(OH)_5$) powder was obtained. The obtained powder sample was analyzed by scanning electron microscopy (SEM, JCM-5100, JEOL, Tokyo, Japan), and powder X-ray diffraction meter (XRD, UltimaIV, Rigaku, Tokyo, Japan). The amount of Zn^{2+} ions released from powder sample was measured as follows; the powder was dispersed in physiological saline at 37 °C for 1 week. The Zn^{2+} ions released

in the saline was measured by inductively coupled plasma-mass spectroscopy (ICP-MS, ELAN DRCII, Perkin Elmer Japan Co., Ltd., Kanagawa, Japan).

Animal experiment

The animal committee of Yamagata University, Yamagata, Japan approved the protocols for the animal experiment described in this study. Six male SD-rats (CLEA Japan,Inc., Tokyo, Japan), weighting 345±42 g, were used in the study. The animals received an inhalation dose of the general anesthesia with 3% sevoflurane (Maruishi Pharmaceutical Co., Ltd, Osaka, Japan) and then were sedated with an intramuscular injection of xylazine hydrochloride (Sedeluck, Nippon Zenyaku Kogyo Co., Ltd, Fukushima, Japan). After abdominal hair was removed, the skin was disinfection with 7% povidone-iodine. Lidocaine hydrochloride with epinephrine (Xylocaine Poly Amp 2%, Fujisawa Pharmaceutical Co., Ltd, Osaka, Japan), a local anesthetic, was administered close to the portion creating skin defects. Skin defects with a 10 mm diameter were made on the abdomen. The control group was covered with commercial wound dressing material (Duoactive ET®, Convatec Inc., USA). In contrast, ZnO and $Zn_5(CO_3)_2(OH)_5$ groups were applied with 0.005 g of corresponding powder and then covered with the same commercial wound dressing material as the control wounds. The evaluation was conducted at 1-and 2-week intervals. The details of animal experiments refer to the literatures [7,8].

Digital photograph of the wounds was taken at 0, 1, 2, and 4 weeks. The area of the wounds was measured from the captured images using an image-processing program (Image J, National Institutes of Health, Bethesda, USA). The values measured by the program were used for calculating the residual wound area of each image. The percentage of reduced wound area was calculated by the following equation (1):

$$\text{Percentage of residual wound area} = \frac{W_0}{W_t} \times 100 \quad (1)$$

Here, W_0 and W_t represent the initial wound area and the wound area measured at 1, 2, and 4 weeks, respectively. For each parameter, the mean value (±) was calculated, and the percentage of reduced wound size was evaluated by one-way Welch's *t*-test for statistical significance at a significance level of 5% (p value < 0.05). The error bar represents the standard deviation (SD).

Skin tissues including wounds were collected at 1 and 2 weeks for histological evaluation. The excised tissues were fixed and then embedded in a paraffin wax block. The specimens were sectioned into 6-8 μm thicknesses. The sections were stained using hematoxylin and eosin staining (HE staining, Muto Pure Chemicals, Co. LTD, Tokyo, Japan).

RESULTS

Material evaluation

Figure 1 shows the XRD pattern and SEM image of ZnO. The XRD pattern corresponding to ZnO with hexagonal structure was detected (Figure1A). SEM observation shows that ZnO powder was composed of polygonal particles of 0.2 to 1 μm in size (Figure 1B). The XRD pattern and SEM image of $Zn_5(CO_3)_2(OH)_5$ are shown in Figure 2A and B, respectively. The detected XRD peaks were consistent with monoclinic $Zn_5(CO_3)_2(OH)_5$. The particle in $Zn_5(CO_3)_2(OH)_5$ powder was size in the range of 0.05-0.1 μm, observing as a cotton-like shape with interlinked particles.

Table 1 summarized the pH value of saline dispersed with powder sample and the concentration of Zn^{2+} ions released from powder sample. The pH value in ZnO and $Zn_5(CO_3)_2(OH)_5$ was 7.6 and 7.8 in weak alkalinity, respectively. Generally, the pH value in intracellular is in the range from 6.8 to 7.4, and the pH value of both samples were found to be slightly higher than intracellular pH values. On the other hand, the concentration of Zn^{2+} ions released from $Zn_5(CO_3)_2(OH)_5$ was 11.3 μmol/L, which was about one quarter of the concentration released from ZnO. That is, the solubility of $Zn_5(CO_3)_2(OH)_5$ in the saline was thought to be lower than that of ZnO.

Evaluation of regenerated tissue

The digital photographs of the wound after each healing time were shown in Figure 3. At 1 week, the formation of the white tissue without elasticity was observed at the wound site in the ZnO group. In contrast, the control and $Zn_5(CO_3)_2(OH)_5$ groups showed the formation of bright red tissue. At 2 weeks, wound astringent was recognized in all groups but white tissue remained slightly in the ZnO group. To investigate why white granulation was observed in the ZnO group, HE-stained image was acquired at high magnification at the wound site and measured by a micro-Raman spectrometer.

Figure 4 shows HE-stained images and Raman spectra of white tissue formed by applying ZnO powder to the wound for 1 week. As shown in Figure 4A, bulks stained a dark red with eosin were observed in white tissue. Then, Raman spectroscopy was performed on the bulks. Raman spectra were detected as the peak at 330, 380, 410, 440, and 540 cm^{-1} (Figure 4B). The Raman spectra detected were consistent with those of ZnO reported already [9]. In the $Zn_5(CO_3)_2(OH)_5$ group, there was no the powder residue in the regenerated tissue.

The residual wound area with healing time was shown in Figure 5. Residual wound area decreased with the healing time in all groups. In 1 week, there was no significant difference between the groups. After a healing time of 2 weeks, however, a significant difference was found between the groups, with the $Zn_5(CO_3)_2(OH)_5$ group having the smallest residual wound area. The residual wound area in the ZnO group was significantly larger than in the control and $Zn_5(CO_3)_2(OH)_5$ groups.

Figure 6 shows HE-stained skin in the wound healing site at each healing time. At the wound healing site after 1 week, the infiltration of inflammatory cell such as neutrophils and lymphocytes as well as neovascularization was observed in all groups. Observation of the wound healing site after 2 weeks showed that the infiltration of inflammatory cells in the ZnO group was similar to that at 1 week. In contrast to the ZnO group, the infiltration of inflammatory cells in the control and $Zn_5(CO_3)_2(OH)_5$ groups was suppressed compared to 1 week, and a large number of fibroblasts were recognized, but not in the ZnO group.

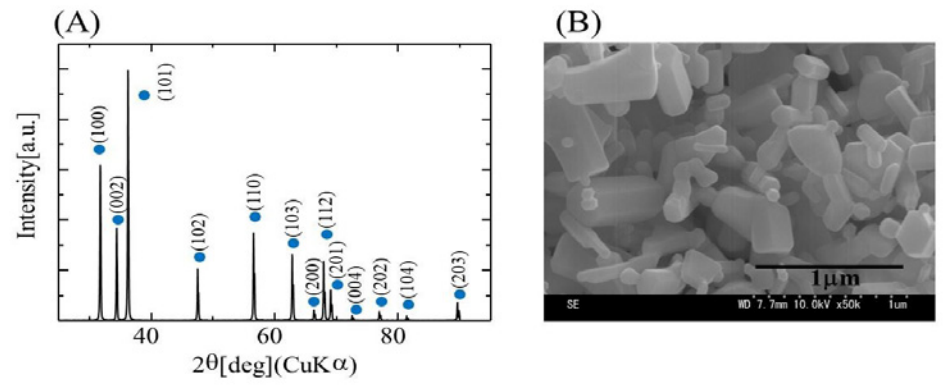

Figure 1 XRD pattern (A) and SEM micrograph (B) of the ZnO powder used in this work.

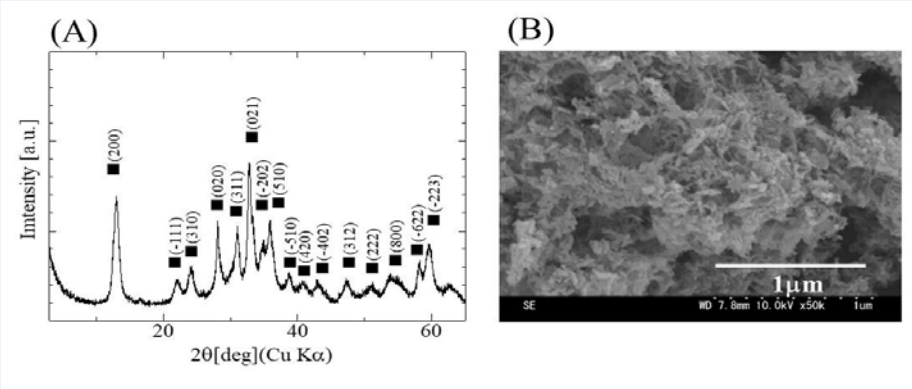

Figure 2 XRD pattern (A) and SEM micrograph (B) of the Zn5(CO3)2(OH)5 powder used in this work.

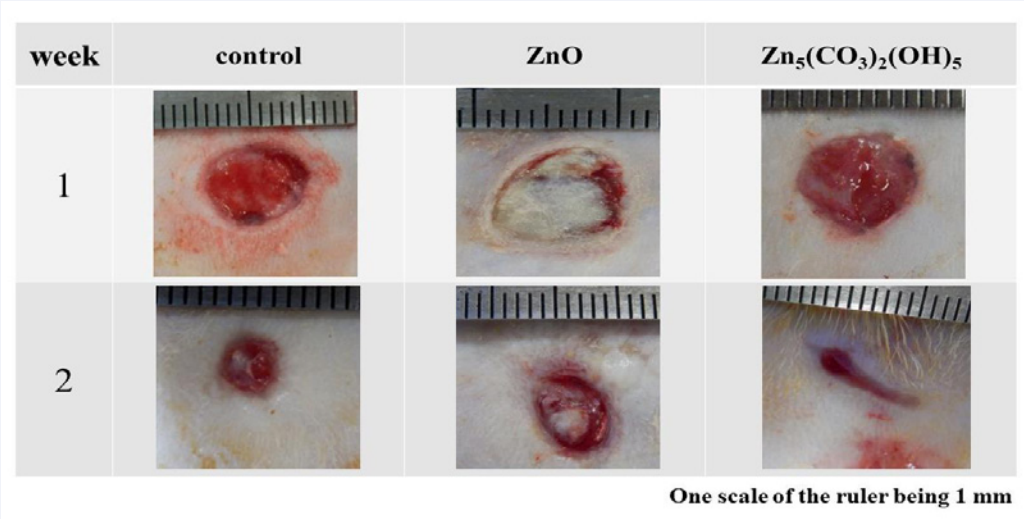

Figure 3 Gross observations of the wounds in the control, ZnO, and Zn5(CO3)2(OH)5 Groups at each healing time.

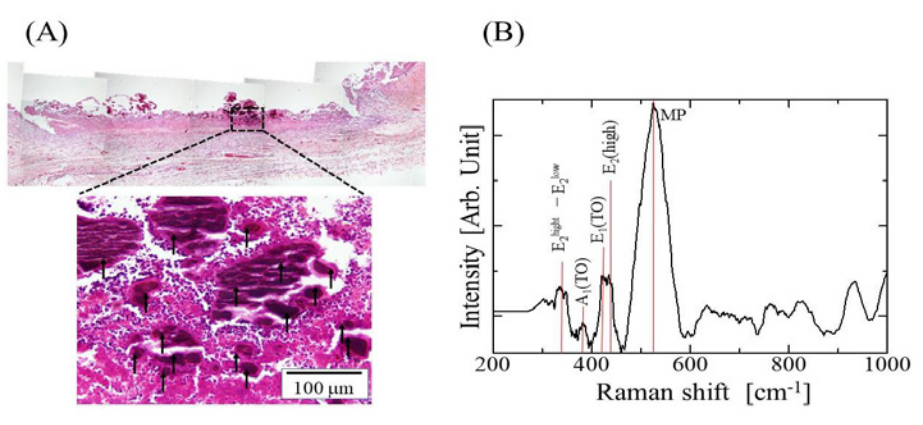

Figure 4 HE stained images (A) of poor granulation tissue and Raman spectrum (B) of the ZnO observed in the tissue.

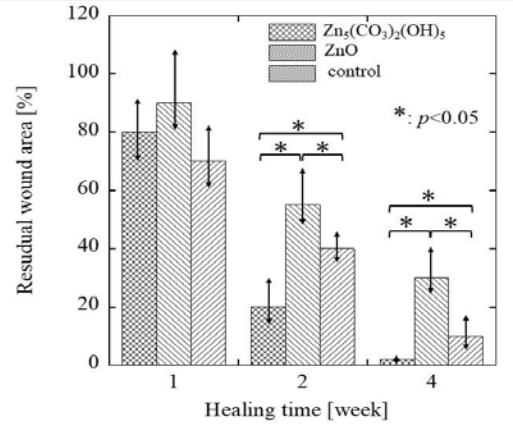

Figure 5 Percentage of residual wound area with healing time in the control, ZnO, and Zn5(CO3)2(OH)5 groups.

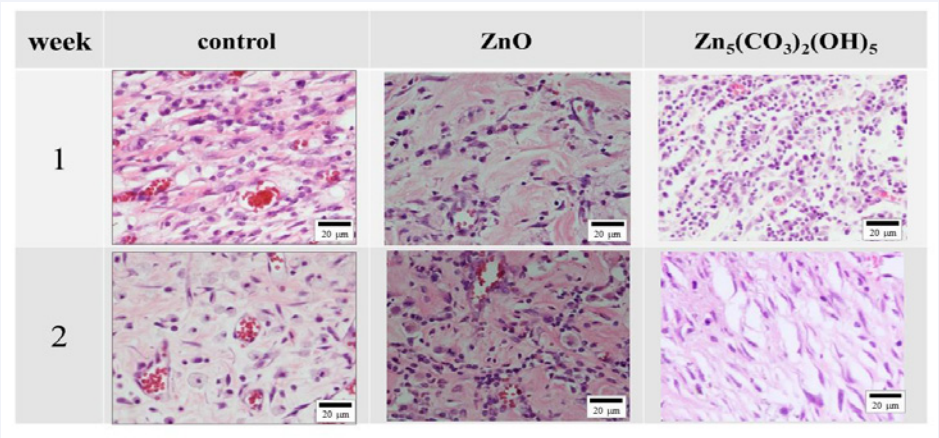

Figure 6 The images of HE-stained skin at each healing time in the control, ZnO, and Zn5(CO3)2(OH)5 groups.

Table 1: The pH values in the ZnO and $Zn_5(CO_3)_2(OH)_5$, and the concentration of Zn^{2+} ions released from these powders for 1 week.

Characterization	ZnO	$Zn_5(CO_3)_2(OH)_5$
pH	7.6	7.8
Zn^{2+}ion released from powder (mol/L)	43.7	11.3

DISCUSSION

Granulation tissue has been classified into benign granulation showing a bright red due to abundant blood flow, poor granulation showing a white with low blood flow and abnormal collagen formation, and necrotic granulation showing a black due to cell necrosis [10]. Therefore, the white tissue observed in the ZnO group was presumed to be poor granulation. Poor granulation has been reported to be formed by foreign body reactions, cytotoxicity, and acute inflammation [11]. The pH value of physiological saline dispersed with powder sample at 37°C was 7.6-7.8, which was in the range of the optimal pH value for keratinocyte and fibroblast proliferation. ICP-MS detected that the concentration of Zn^{2+} ions released from ZnO and $Zn_5(CO_3)_2(OH)_5$ was 43.74 and 11.3 μmol/L at 37°C for 7 days, respectively. The inhibitory concentration of Zn^{2+} ions on cell proliferation has been reported to be greater than 500 μmol/L [12]. In the powder sample used, the concentration of Zn^{2+} ions were smaller than the inhibitory value reported, which was presumed to be non-cytotoxic. From Raman spectroscopy, ZnO powder was found to remain in poor granulation. The reason why ZnO powder caused poor granulation was supposed to be acute inflammation due to foreign body reactions with residual ZnO powder in the tissue.

Skin regeneration and healing proceed in the following order: the inflammatory phase, proliferative phase, and remodeling phase. Wound healing in the ZnO group was delayed compared to the control and $Zn_5(CO_3)_2(OH)_5$ groups, being observed on the infiltration of the inflammatory cells at the regenerated tissue for 2 weeks. In other words, it was presumed that the stage of wound healing in ZnO group was likely to be the inflammatory phase. In the case of control group (commercial wound dressing), inflammatory cell infiltration and fibroblasts were observed at 2 weeks, suggesting that there was a transitional stage between the inflammatory and remodeling phases. In the $Zn_5(CO_3)_2(OH)_5$ group, inflammation ceased and mainly fibroblasts were observed at 2 weeks, suggesting that wound healing was in the proliferative phase. Furthermore, wound site closure in the $Zn_5(CO_3)_2(OH)_5$ group occurred earlier than in the control and ZnO groups. In these results, $Zn_5(CO_3)_2(OH)_5$ was indicated to have a higher wound-healing effect than ZnO and commercial wound dressing. The significant effect of $Zn_5(CO_3)_2(OH)_5$ on wound healing was supposed to be due to the pharmacological action of Zn^{2+} ions without sustained inflammation based on foreign body reactions.

CONCLUSION

In the present work, the wound healing effect between medicinal zinc oxide and hydrozincite was compared using a rat model. Zinc oxide resulted in prolonged wound healing by causing inflammation due to foreign body reactions. Hydrozincite was clarified to have a higher wound-healing effect than ZnO and commercial wound dressing. Hydrozincite powder can be expected as an effective ceramic powder alternative to zinc oxide powder in zinc oxide ointments.

REFERENCES

1. Ågren MS, Phothong N, Burian EA, Mogensen M, Haedersdal M, Jorgensen LN. Topical Zinc Oxide Assessed in Two Human Wound-healing Models. Acta Derm Venereol. 2021; 101: adv00465.
2. Nagajyothi PC, Cha SJ, Yang IJ, Sreekanth TVM, Kim KJ, Shin HM. Antioxidant and anti-inflammatory activities of zinc oxide nanoparticles synthesized using Polygala tenuifolia root extract. J Photochem Photobiol B. 2015; 146: 10-7.
3. Barceloux DG. Zinc. J Toxicol Clin Toxicol. 1999; 37: 279-92.
4. Sobczak AIS, Samantha JP, Stewart AJ. Influence of zinc on glycosaminoglycan neutralisation during coagulation. Metallomics. 2018; 10: 1180-1190.
5. Schwartz JR, Marsh RG, Draelos ZD. Zinc and Skin Health: Overview of Physiology and Pharmacology. Dermatol Surg. 2005; 31: 837-47.
6. Hershfinkel M. The Zinc Sensing Recepter, ZnR/GPR39, in Health and Disease. Int J Mol Sci. 2018; 19: 439.
7. Sasaki Y, Sathi GA, Yamamoto O. In vivo evaluation of wound healing property of zinc smectite using a rat model. J Ceram Soc Japan. 2016; 124: 1199-1204.
8. Sasaki Y, Sathi GA, Yamamoto O, Wound healing effect of bioactive ion released from Mg-smectite. Mater Sci Eng C Mater Biol Appl. 2017; 77: 52-57.
9. Marin O, Soliz T, Gutierrez JA, Tirado M, Figueroa C, Comedi D. Structural, optical and vibrational properties of ZnO:M (M=Al3+ and Sr2+) nano and micropowders grown by hydrothermal synthesis. J. Alloys Compd. 2019; 789: 56-65.
10. Morton LM, Phillips TJ. Wound healing and treating wounds: Differential diagnosis and evaluation of chronic wounds. J Am Acad Dermatol. 2016; 74: 589-605.
11. Anderson JM, Rodriguez A, Chang DT. Foreign body reaction to Biomaterials. Semin Immunol. 2008; 20: 86-100.
12. Lansdown ABG, Mirastschijski U, Stubbs N, Scanlon E, Agren MS. Zinc in wound healing: Theoretical, experimental, and clinical aspects. Wound Repair Regen. 2007; 12: 2-16.